

Bio-Based Tannin-Furanic-Silk Adhesives: Applications in Plywood and Chemical Cross-linking Mechanisms

Emanuele Cesprini, Johannes Jorda, Marco Paolantoni, Luca Valentini, Primož Šket, Valerio Causin, Diana E. Bedolla, Michela Zanetti, and Gianluca Tondi*



Cite This: <https://doi.org/10.1021/acscapm.3c00539>



Read Online

ACCESS |



Metrics & More



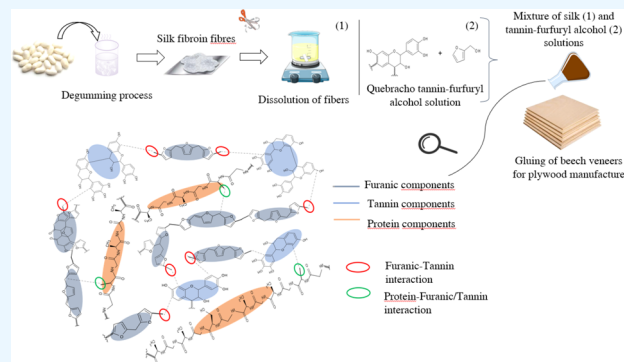
Article Recommendations



Supporting Information

ABSTRACT: Wood polyphenolic extracts, commonly called tannins, are excellent candidates for the production of bioplastics due to their abundance in nature, their commercial availability, and their reactivity. In particular, they were tested as wood adhesives with several hardeners, but their low moisture resistance and their rigidity reduced their technological interest. In the present study, we combined regenerated silk (RS) with tannin-furanic formulations to improve their properties. Three-layer plywood glued with these several fully renewable tannin-silk-furanic adhesives were tested for their mechanical properties: the modulus of elasticity, the modulus of rupture, and both dry and wet shear strength were enhanced when 20 wt % of RS was added. Initially, the cross section of the prepared samples was investigated by scanning electron microscopy, indicating a good dispersion of RS within the tannin-furanic matrix. Afterward, thermomechanical analysis of the adhesive highlighted that RS slows down the polymerization rate, decreasing the cross-linking kinetics of polyfurfuryl alcohol. Chemical investigations through ATR-FTIR and ^{13}C -NMR show the formation of covalent bonds between RS and the furanic matrix. In summary, the combination of bioresources from the vegetal and animal kingdom allows the manufacturing of fully bio-based adhesives with enhanced mechanical properties and water resistance. This represents an important breakthrough in the exploitation of polyphenols, opening perspectives for their application in material science.

KEYWORDS: regenerated silk, protein, fibroin, flavonoids, furanic, engineered wood products, sustainable



INTRODUCTION

Reducing the dependence on fossil derivatives has become a worldwide issue due to the necessity to restrain global warming and develop a sustainable economy.¹ For instance, the plastics field accounts for 5–7% of the consumption of oil derivatives, releasing more than 850 million tons of CO_2 into the atmosphere.² Specifically, the higher greenhouse gas emissions in the plastic manufacturing industry are related to the raw material extraction process (e.g., 61%) followed by the polymer production (e.g., 30%).³ It has been estimated that replacing approximately 66% of conventional plastics with bio-based alternatives would avoid between 241 and 316 MtCO_2 equivalents per year,⁴ thus explaining the need to seek sustainable alternatives to oil derivatives. Although the most common commercial plastics are still made from oil derivatives, the same materials may also be replaced by renewable resources. Monomers or also biopolymers can be obtained from nature with the goal of replacing synthetic plastic such as polyethylene or polypropylene.⁵ Tannins, which are wood extracts of polyphenolic nature, have been shown to be very attractive and perform well for multiple purposes. These substances are produced by plants to protect the

lignocellulosic body against biological and radiation attacks due to their chemical structure and antioxidant capacity.⁶ Furthermore, they have a 'green' extraction process through the use of water as a solvent under moderate pressure and temperature.⁷ Tannins are extracted industrially and are therefore abundantly available because they have been used as tanning agents in the leather tannery row because of their strong complexing power with proteins.⁸ In addition to this, tannin extracts have been used for medical purposes as antioxidants and free radical scavengers.⁹ In the last 2 decades, due to their appealing chemical features, tannins have been used to produce bio-based plastics, with particular interest for insulation foams,^{10–12} wood preservatives,^{13,14} and wood adhesives.^{15,16} The addition of mainly synthetic-based cross-linkers such as hexamine, formaldehyde, or glyoxal leads to

Received: March 27, 2023

Accepted: May 4, 2023

stable three-dimensional thermosetting polymers.^{17,18} Despite the appealing features of the aforementioned tannin-based formulation, concerns about health problems and the need for detachment from oil derivatives have led the research to promote formaldehyde-free fully renewable formulations as a profitable source for greener products. In this direction, furfuryl alcohol is a bio-derived material which is mainly obtained from the hydrogenation of furfural, which is itself a derivative of the dehydration of agricultural and forest waste from hemicelluloses.¹⁹ The ability of furfuryl alcohol to self-cure under acidic conditions^{20,21} enables the design of different materials applicable in the field of engineered wood products, including impregnation²² and modification²³ of woody materials. Moreover, due to the resistance to acid, alkali, high temperature, fungal attack, and corrosion²⁴ and because of its good interaction capacity with tannins,²⁵ furfuryl alcohol can be involved as a green cross-linker to produce a fully renewable copolymer.^{26,27} However, some critical drawbacks of furanic-tannin copolymers like poor moisture resistance²⁸ and high rigidity²⁹ still limit the application. Hither, proteins have attracted great attention due to their renewability, effortless modification, biodegradability, and abundance.³⁰ Although the use of protein-based adhesive resins alone does not allow for high performance,³¹ the combination of these with other resources, as tannins or furanic derivatives, has led to satisfactory results in the wood adhesive sector.^{32,33} Silk fibroin (hereinafter named regenerated silk, RS) is one of the most promising natural protein-based biomaterials due to its inspiring biodegradability and superior mechanical performance.³⁴ Such a biopolymer recovered from insect farming [*Bombyx mori* (*B. mori*) silkworms] can be processed in solution to enable the fabrication of adhesives with tunable mechanical properties,³⁵ opening up alternatives to the main plant proteins currently proposed.^{36,37}

In this study, the effect of adding different amounts of RS into tannin-furfuryl alcohol formulations for plywood manufacturing was investigated. Further, the interaction between the components of the adhesive was observed during and after curing through thermomechanical analysis (TMA) and solid-state ¹³C-NMR Fourier transform infrared (FTIR) spectroscopy.

MATERIALS AND METHODS

Materials. Quebracho (*Schinopsis balancae*) tannin extract (Fintan 737B) was kindly provided by the company Silvateam (S. Michele Mondovi, Cuneo, Italy), while furfuryl alcohol (99%) was provided by International Furan Chemical IFC (Rotterdam, The Netherlands). Lowest grade *Bombyx mori* silk cocoons were provided by a local company (CREA-AA, Padova, Italy). Sodium hydrogen carbonate, calcium chloride, and formic acid were supplied by Alfa Aesar (Thermo Fisher, Waltham, MA, USA). Preconditioned (20 °C, 65% relative air humidity) rotary cut defect-free beech (*Fagus sylvatica*) veneers, purchased from Europlac (Topolcany, Slovakia), with a nominal thickness of 2.2 mm, density of 0.72 g/cm³, and 12% m.c., were used to prepare the three-layer plywood.

Synthesis of Adhesive. The silk fiber dissolution method was carried out according to previous work.³⁸ Briefly, *B. mori* silk cocoons (5 g) were degummed in boiling water (300 mL) at 1.7% of NaHCO₃ for 30 min and flushed with deionized water, and the procedure was repeated twice. The degummed silk fibers were dried at room temperature under air flux and then dispersed into the formic acid/calcium chloride solution by magnetic stirring at room temperature for 5 min until a homogeneous solution was obtained. The amount of calcium chloride was defined as a function of silk content. The silk-calcium chloride weight ratio was set at 70:30, while a silk

concentration of 0.11 g/mL in formic acid was chosen. Meanwhile, a tannin-furfuryl alcohol solution was prepared at room temperature under mechanical stirring at a fixed weight ratio of 60:40. Afterward, the two solutions were mixed and mechanically stirred at different RS concentrations calculated on fixed solid tannin content, obtaining different tannin-furfuryl alcohol formulations (TFS). The RS content was varied from 10 wt % up to 30 wt %. The composition of the formulations is reported in Table 1.

Table 1. Relative Content of each Component within the Final Formulations

samples	tannin (wt %)	furfuryl alcohol (wt %)	RS (wt % on tannin)
TFS-0	60	40	/
TFS-10			10
TFS-15			15
TFS-20			20
TFS-30			30

Plywood Manufacturing. The plywood lay-up consisted of three-layered 90° cross-wise oriented 2.2 mm thick beech veneers. Adhesive application was carried out manually by weighing 200 g/m² of adhesive per glue line. Pressing was conducted using a Höfler HLOP 280 (Taiskirchen, Austria) hot press. The pressing conditions were set as follows: pressure of 3 N/mm², temperature of 125 °C, and 15 min of pressing time. The as-prepared boards were stored until constant weight in a climate chamber at 20 °C and 65% relative humidity. Test specimens were cut from the plywood boards for the determination of bending strength [modulus of rupture (MOR)], stiffness [modulus of elasticity (MOE)], and dry and wet tensile shear strength (SS).

Mechanical Characterization. Dry-state SS and 24 h water soaking tensile SS were determined according to EN 314:2004³⁹ with specimen dimensions 100 mm × 25 mm. MOR and MOE were determined by a three-point bending test according to EN 310:1993 with specimen dimensions 250 mm × 50 mm.⁴⁰ All mechanical properties (SS, MOE, and MOR) were determined using a Zwick/Roell 2508497.04.00 universal testing machine (Ulm, Germany).

SEM. The morphological characterization of the adhesives was performed by scanning electron microscopy (SEM) with an FEI Quanta scanning electron microscope (variable pressure environmental E/SEM). The instrument was also equipped with EDX (EDAX Element-C2B) for X-ray detection. The images were recorded at 20 kV.

TMA. TMA was carried out with a TMA/SDTA840 Mettler Toledo (Mettler Toledo, Columbus, OH, USA) instrument equipped with a three-point bending probe. About 20 mg of tannin-based formulations (TFS-0, TFS-10, TFS-15, TFS-20, and TFS-30) were applied between two beech wood plies (15 mm × 5 mm × 1.5 mm). Isothermal and nonisothermal methods were applied: the former was run at 25 °C for 240 min, while the latter consisted of 10 °C/min heating rate from 40 to 200 °C. For both methods, a cycle of 0.1/0.5 N force was applied on the specimens, with each force cycle lasting 12 s (6 s/6 s).

In order to investigate the chemical bonding evolution, different spectroscopic investigations were performed on polyfurfuryl alcohol (PFA) cross-linked in formic acid and RS obtained by dissolution in formic acid. PFA-RS and PFA-RS-quebracho tannin (PFA-RS-T) were acquired and compared with the cured mixed formulation subject of this study.

¹³C-NMR Solid-State Analysis. Solid-state ¹³C-NMR experiments were performed on a Bruker AVANCE NEO 400 MHz NMR spectrometer using a 4-mm CP-MAS probe. The sample spinning frequency was set to 15 kHz experiments consisting of excitation of protons with p/2 pulse of 3.0 s, CP block of 2 ms, and signal acquisition with high-power proton decoupling. A total of ca. 2000 to 14,000 scans were accumulated with the repetition delay of 5 s.

ATR-FTIR Analysis. FTIR spectra measurements were done in the attenuated total reflection (ATR) mode using an Alpha (Bruker

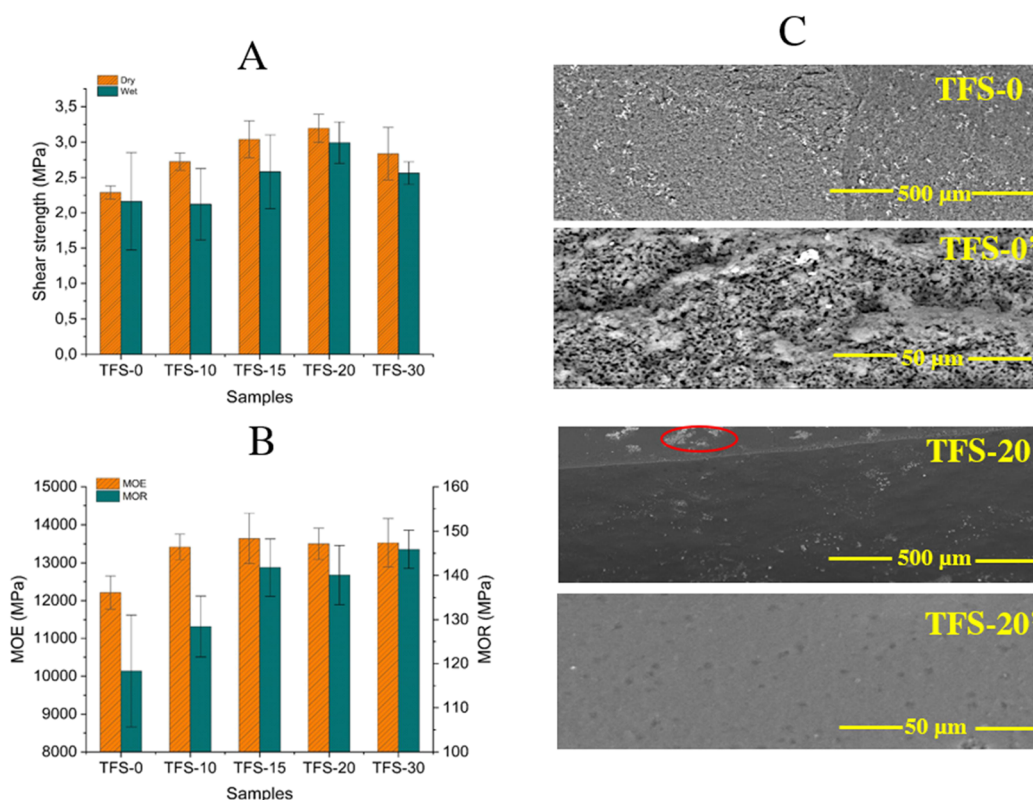


Figure 1. (A) Dry and 24 h wet SS of reference panels (TFS-0) and TFS samples synthesized at different wt % of RS. (B) MOE and MOR of reference panels (TFS-0) and TFS samples synthesized at different wt % of RS. (C) SEM images of TFS-0, TFS-20 and TFS-0', TFS-20' samples at different magnifications (e.g., $\times 100$ and $\times 1000$, respectively).

Optics) spectrometer equipped with a Platinum ATR module. The spectra were registered in the range between 400 and 4000 cm^{-1} , averaging over 30 scans with a resolution of 2 cm^{-1} . The spectra were then baseline-corrected, normalized, and smoothed with the RStudio Team (2021) software.

FTIR. FTIR hyperspectral images were acquired by using a bidimensional 64×64 pixels focal plane array coupled to a VIS-IR Hyperion 3000 (Bruker Optics, Billerica, US) microscope and with a VERTEX 70v in-vacuum interferometer (Bruker Optics, Billerica, US) through a $15\times$ Cassegrain objective-condenser pair in the transmission mode. Slices of 10 μm of PFA-tannin and PFA-tannin-silk were prepared with a rotary microtome (Leica RM2245; Leica Biosystems, Nussloch, Germany), so that the samples could be measured in the transmission mode. For each tile, 4096 spectra were acquired with 256 scans at a spectral resolution of 4 cm^{-1} . Data were corrected for water vapor using Opus 8.5 SP1 (Bruker Optics, Billerica, US) and then analyzed using Quasar (<https://quasar.codes>).^{41,42} All spectra were vector-normalized, cut in the region 1850–850 cm^{-1} , and baseline-corrected with the rubber band correction. Integration was calculated on the average spectra of the whole tile (4096 scans) of each sample with the height of the band around 1715 and the band around 1520. Finally, its ratio was estimated and compared.

Statistical Analysis. Analysis of variance (ANOVA) was used to assess significant differences between the investigated formulations through one-way ANOVA and Kruskal test, depending on whether the data are normally or non-normally distributed, respectively. Any groups that showed a significant difference were discriminated according to the Tukey multirange test for ANOVA or Dunn test for Kruskal, and a 95% confidence level was selected. Statistical analysis was performed using RStudio Team (2021). Kruskal-Wallis multiple comparison p -values were carried out to analyze the correlation between MOR of the fabricated adhesives because of non-normal data distribution.

RESULT AND DISCUSSION

The mechanical properties of the three-layer plywood are depicted in Figure 1A,B. In the production of multilayer panels, one of the key parameters refers to the glue line property, which shall guarantee sufficient adhesion for the final stability of the panel. The most significant physical indicator is the SS in both wet and dry conditions (Figure 1A). One-way ANOVA reported high correlation between the silk concentration and SS_{dry} (p -value = 6.29×10^{-5}). Specifically, a significant difference (p -value < 0.05) between the reference panel (TFS-0) and TFS-15/20/30 is highlighted by the Tukey test, confirming the higher adhesive property of the TFS-20 sample (e.g., 3.2 MPa). In contrast, any substantial difference between TFS-0 and TFS-10 (p -value = 0.052) was not observed.

After 24 h of water storage at room temperature, the shear stress was evaluated, and the tendency is reported by the red curve in Figure 1A. The addition of RS to the tannin-furfuryl alcohol matrix led to an increase in panel stability (p -value = 0.0261), reaching its highest value (e.g., 2.8 MPa) for the TFS-20 formulation. A proportional increase in the tensile SS is achieved up to 20% of RS, followed by a decrease when the RS concentration reaches 30%. Although the stability of the adhesive reaches its best properties at 20 wt % of RS, the results obtained are all compliant for dry condition purposes according to European standards that set the wet SS above 1 MPa.³⁹ The effect of RS addition on both MOE and MOR was investigated and is reported in Figure 1B. The addition of RS increases the values of both MOE and MOR. Specifically, the RS addition affects the MOE (p -value = 0.0144), showing a significant change between the reference panels (TFS-0) and

those where RS was added (p -value < 0.05). Otherwise, no differences in MOE were highlighted by increasing the RS content (p -value > 0.05). Finally, the silk addition positively affects the mechanical properties, registering a p -value of 0.0043 for MOR. Similarly, when silk was added, an increase of the MOR from 128 to 146 MPa was recorded.

Focusing on the critical tensile SS parameter, the comparison of the current formulations with literature studies highlighted the competitiveness of this adhesive resin.

In particular, the use of fully renewable tannin-furfural adhesives showed poor moisture resistance.²⁹ Indeed, although a dry shear stress strength between 1.7 and 2.3 MPa is registered, the formulation denoted no resistance to moisture due to the panel delamination during the 24 h water soaking for plywood EN 314 class 1 application.²⁹ The grafting of counterparts to the tannin base skeleton is therefore necessary to achieve competitive properties. In this way, the inclusion of oxidized glucose to mimosa tannin allowed dry SS between 1.4 and 2.0 MPa, increasing the moisture resistance until 0.3–0.5 MPa after 24 h water soaking.⁴³ Chen and co-workers reported a wet tensile SS of 1.1 MPa for soybean meal (SM) flour, larch tannin, and triglycidylamine adhesive formulation.⁴⁴ Similar results were reported by Zhou et al.,⁴⁵ who achieved dry and wet SSs of 2.1 and 1.6 MPa, respectively, building a complex structure of layered double hydroxide, anchored chicken feather fiber, tannic acid, and SM. The combination of PFA with gluten proteins showed good bonding properties, achieving a shear strength after 24 h in cold water of about 0.9 MPa.³² Good strength was also reported for 3 h in boiling water.³²

Another interesting natural resource of polyphenolic character is lignin, which is also used in combination with different kinds of proteins to produce plywood boards. On this note, Pang et al.⁴⁶ and Liu et al.⁴⁷ reported lower values of both SS_{dry} and SS_{wet} than the results reached by the proposed tannin silk formulation, which displayed to be competitive with phenol-formaldehyde (PF)-bonded plywood too.⁴⁸

Moreover, in terms of MOE and MOR, the current formulation has shown properties comparable with the main synthetic adhesives. Indeed, Jorda et al. reported for epoxy, urea-formaldehyde, melamine-urea-formaldehyde, phenol-formaldehyde, and polyurethane resins bonded five-layer beech (*Fagus sylvatica*) plywood an MOE between 9500 and 11,700 MPa, while for MOR the values fall between 95 and 115 MPa.⁴⁹ Additionally, Biadala et al.⁵⁰ reported a mean MOE of 13,720 MPa for three-layered PF-bonded beech plywood and an MOR of 158.4 MPa. Thus, with an MOE over 13,000 MPa and MOR beyond 140 MPa, the copolymers of furfuryl alcohol-tannin-fibroin exhibit mechanical properties at least comparable to the main synthetic resins.

The morphology of the reference (TFS-0) and TFS-20 samples was investigated by SEM analysis as reported in Figure 1C. The TFS-0 and TFS' show a jagged morphology due to the fast evaporation of formic acid during the cross-linking. On the contrary, the addition of RS (TFS-20 and TFS-20') results in a more compact material. Salt crystals, for example, $CaCl_2$, are visible along with the appearance of RS agglomerates (red cycle in Figure 1C, TFS-20' sample, and Figure S1 in the Supporting Information section).

In order to understand and correlate the different formulations and their reactivity, the comparison between the reference and the silk-added samples was monitored through nonisothermal and isothermal TMA. In Figure 2, the

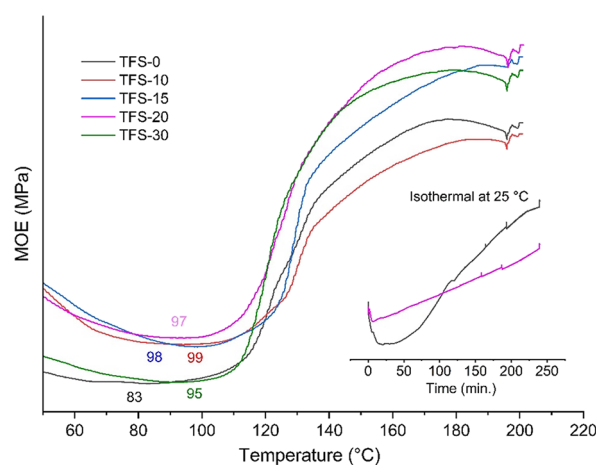


Figure 2. Nonisothermal and isothermal (see the inset) mechanical analyses of TFS-0 and TFS samples synthesized at different wt % of RS.

thermomechanical behavior of formulations described in Table 1 is reported. Focalizing on the nonisothermal method, heat affects the sample behaviors simultaneously in two different ways, namely, by physical and chemical effects.⁵¹ For the former, an increase of temperature leads to the softening and decreases the stiffness of the polymers, which happens to all samples before 80 °C. By increasing the temperature, the chemical effect of cross-linking overcomes the physical one, and an increase in stiffness was registered between 80 and 180 °C due to the starting of the polymerization process.

Although all samples showed a maximum MOE peak around 180 °C, the addition of RS shifts the starting of curing of about 10 °C. This suggests (see below) that the addition of fibroin delays the copolymerization of tannin and furfuryl alcohol. Once the curing process starts, the presence of fibroin accelerates the hardening, and this can be seen by the slope of the thermograms which are particularly visible for the formulation containing at least 15 wt % of RS. However, at the end of the polymerization process, the presence of silk increased the properties of the copolymer. This result supports the observations already considered in the mechanical tests: in this case, the TFS-20 registered the highest MOE compared to the other formulations.

The isothermal curves for TFS-20 and TFS-0 (black and pink) are shown in Figure 2. After 240 min of reaction at room temperature, the reference (TFS-0, black curve) reached a higher MOE value than TFS-20, indicating faster reaction kinetics. The acidity resulting from the presence of formic acid allows for a fast self-polymerization⁵² of furfuryl alcohol as well as copolymerization with tannin.⁵³

¹³C-NMR and ATR-FTIR analyses were performed to understand the chemical interactions occurring between silk and the tannin-furanic matrix.

Many studies involved the characterization of PFA since the last century,^{21,54,55} but the debate is still open due to its utilization as a renewable and abundant material, with more molecular rearrangements that have been proposed over the years.^{25,56,57} In short, there are two reactions occurring: (i) the linear polymerization summarized in Scheme 1A and the (ii) Diels-Alder cross-linking of the ring-opened structures reported in Scheme 1B.

In Figure 3, the ¹³C-NMR spectra of PFA, RS, PFA-RS, quebracho tannin(T), and PFA-RS-T are reported. Comparing

Scheme 1. (A) Principal Mechanism of the Reaction of Furfuryl Alcohol Polymerization; (B) Diels-Alder Reaction Mechanism Involved in the Polymerization of Furfuryl Alcohol

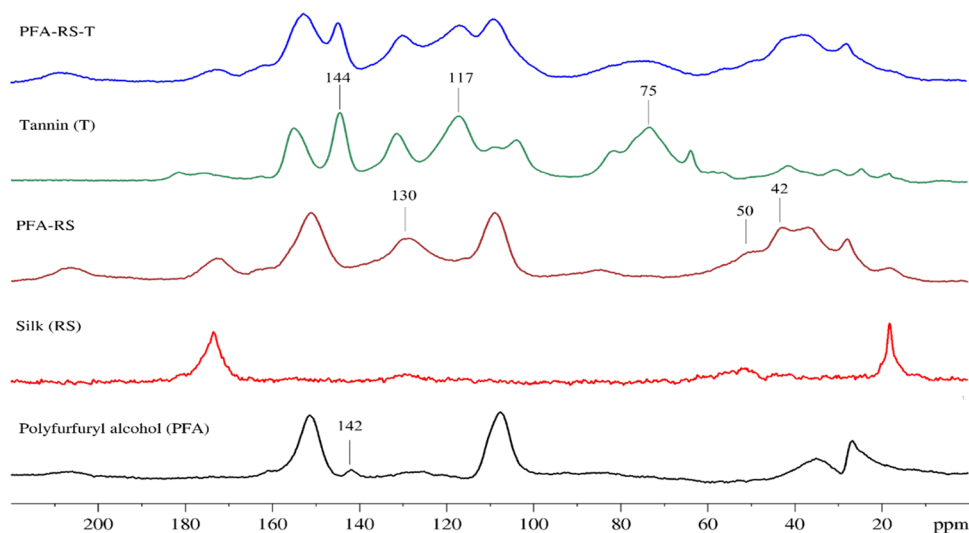
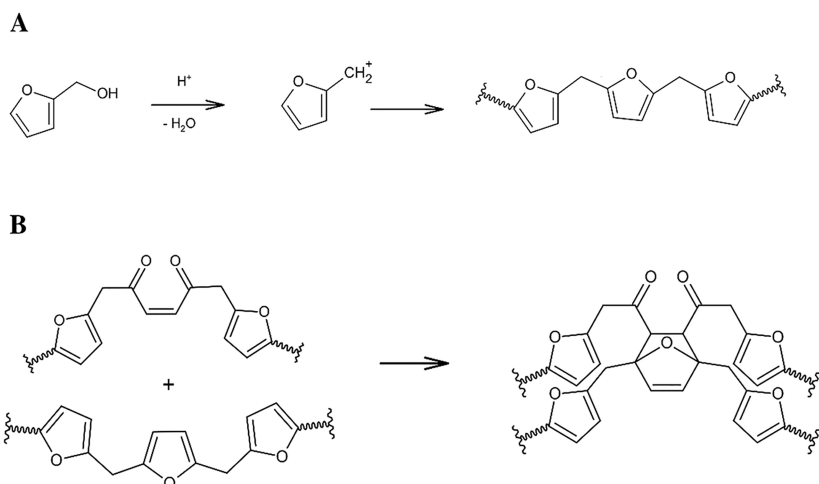


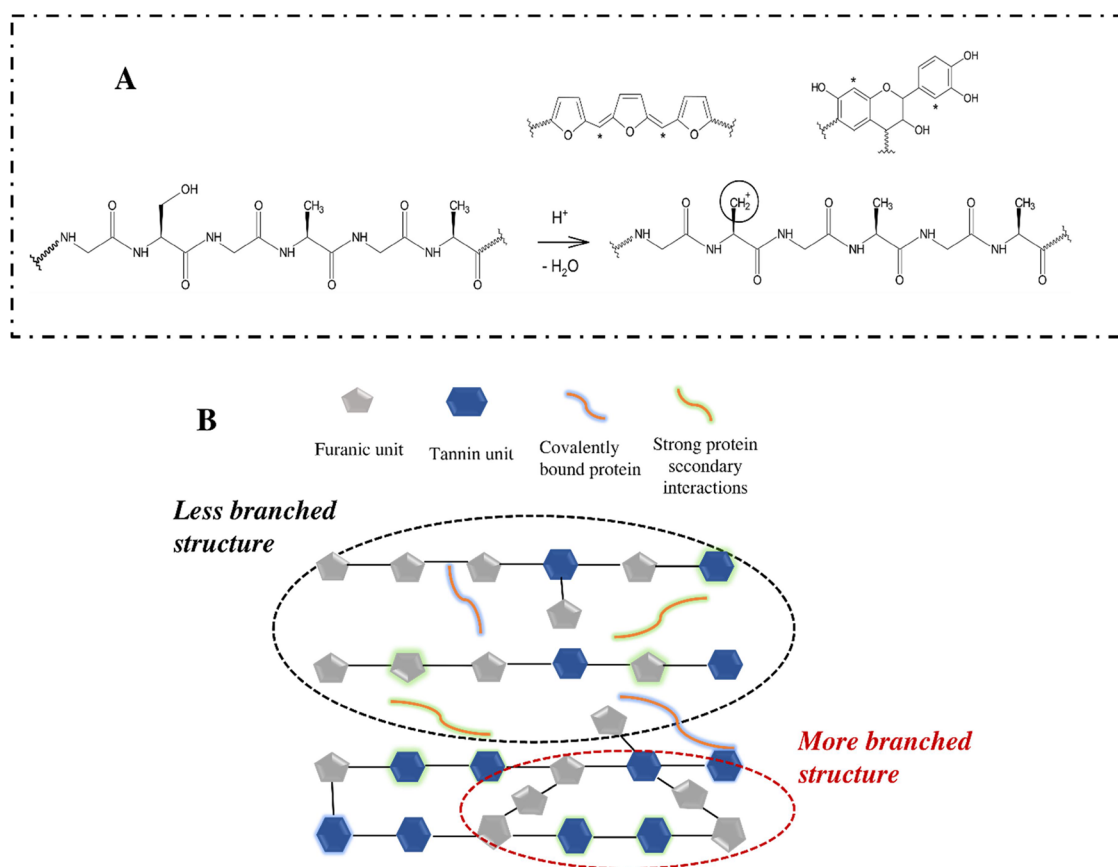
Figure 3. ^{13}C -NMR spectra of PFA (black curve), RS (red curve), PFA-RS (brown), quebracho tannin (T, green curve), and quebracho polyfurfuryl alcohol-regenerated silk-quebracho tannin (PFA-RS-T, blue curve).

the spectra of PFA and PFA-RS, it can be seen that despite many signals obtained by superposition of each component, new or highly enhanced peaks were observed. Indeed, when silk is added (PFA-RS, brown curve), the band at 142 ppm disappears or strongly reduces its intensity, while the peak at around 130 ppm is severely enhanced, and the signal at 50 ppm as well the shoulder at around 40 ppm appear. The signal at 142 ppm related to $-\text{C}=\text{C}-$ in the Diels-Alder bicycle⁵⁶ disappears, suggesting a decrease of the cycloaddition cross-linking mechanism, while the enhancement of the signal at 130 ppm can be attributed to the $\text{C}=\text{C}$ of dienophile reagent (Scheme 1B), which is not involved anymore in the Diels-Alder reaction. On the other hand, between 40 and 50 ppm, a signal is detected in the PFA-RS spectrum, which is probably related to more substituted carbons (e.g., ternary carbon).^{21,25} Indeed, the acidity of the solution may lead to the formation of carbocation $-\text{CH}_2^+$ in the primary alcohol of sericin (Scheme 2A). The silk carbocation may interact with nucleophilic centers as PFA linear conjugated system, whose presence is already confirmed by several authors,^{25,57,58} leading to a final three-dimensional network represented in Scheme 2B. The

coupling between those two species could justify the resonance between 50 and 40 ppm which produces secondary and ternary carbons. Furthermore, in support of what has just been hypothesized, Chen et al. have recently confirmed the formation of covalent bonds between PFA and reactive functional groups of gluten protein.³²

The addition of tannin increases the complexity of the system, and the overlapping of signals does not facilitate the recognition of any interactions. Definitely, the peaks visible at 144 ppm, 117 ppm, and around 75 ppm are related to $-\text{C}-\text{O}$ of B ring, $-\text{C}-\text{C}-$ of A ring, and C aliphatic involved in the polyphenolic structure.^{18,53} On the other hand, the interaction of the silk carbocation with the nucleophilic centers of the aromatic rings cannot be excluded (Scheme 2B). However, a stable network between tannin and RS is also guaranteed by strong hydrogen and hydrophobic interactions of those components.⁵⁹ Thus, the presence of the silk within the network allows a more flexible and elastic system (black circle, Scheme 2B), which is not guaranteed without the protein due to the more branched final structure (red circle, Scheme 2B).

Scheme 2. (A) Possible Carbocation Formation in a Primary Alcohol of the Silk Protein Structure and Interaction with Nucleophilic Centers*; (B) Schematic Representation and Possible Interaction of a Tannin-Alcohol Furfuryl Copolymer and Silk



The samples were also investigated by ATR-FTIR spectroscopy. The spectra are reported in Figure 4.

The spectrum of PFA obtained in the present investigation shows several diagnostic signals already observed in a previous work when PFA was prepared using a similar procedure.⁵⁶ The

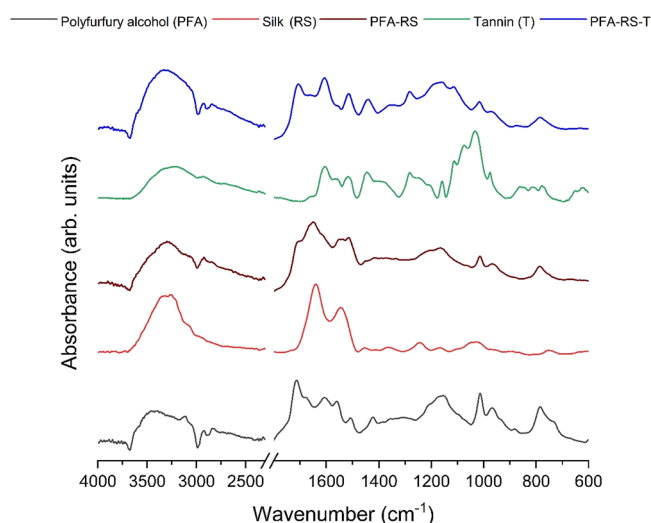


Figure 4. ATR-FTIR spectra of PFA (black curve), RS (red curve), PFA-RS (brown), quebracho tannin (T, green curve), and quebracho polyfurfuryl alcohol-regenerated silk-quebracho tannin (PFA-RS-T, blue curve).

peaks at ca. 1520, 1420, 1013, and 785 cm^{-1} can be ascribed to the linear PFA structure, while the bands at 1715, 1660, and 965 cm^{-1} suggest the presence of the Diels-Alder product within the polymer matrix.⁵⁶ The spectrum of PFA-RS still evidences the signals related to the linear PFA structures at ca. 1520, 1013, and 785 cm^{-1} , the contribution at ca. 1715 cm^{-1} is due to the Diels-Alder product, and the broad band at 965 cm^{-1} is related to ring-opened and/or Diels-Alder structures. Interestingly, it has been proposed that the presence of a contribution at ca. 735 cm^{-1} might be used in conjunction to the peak at 785 cm^{-1} to estimate the relative amount of single-linked and double-linked furan rings within the PFA matrix.⁵⁷ In this respect, the spectra indicate that the relative intensity of the contribution at ca. 735 cm^{-1} decreases going from PFA to PFA-RS, suggesting that the presence of silk reduces the relative fraction of single-linked furan rings. This is consistent with a silk-induced modulation of the cycloaddition cross-linking.

The spectrum of the PFA-RS-T sample is dominated by the tannin contribution; in any case, the signals at 1013 cm^{-1} (linear PFA), 965 cm^{-1} (ring-opened and/or Diels-Alder PFA), and 785 cm^{-1} (linear PFA) can still be recognized. Similar to the case of the binary PFA-RS sample, a contribution at ca. 735 cm^{-1} was not observed, in line with the idea that the silk mainly affects the polymerization process even in the ternary system.

We notice that a carbonyl resonance is still present in the spectrum (1715 cm^{-1}) of the PFA-RS-T sample (blue spectra, Figure 4). This might be attributed to the C=O stretching of

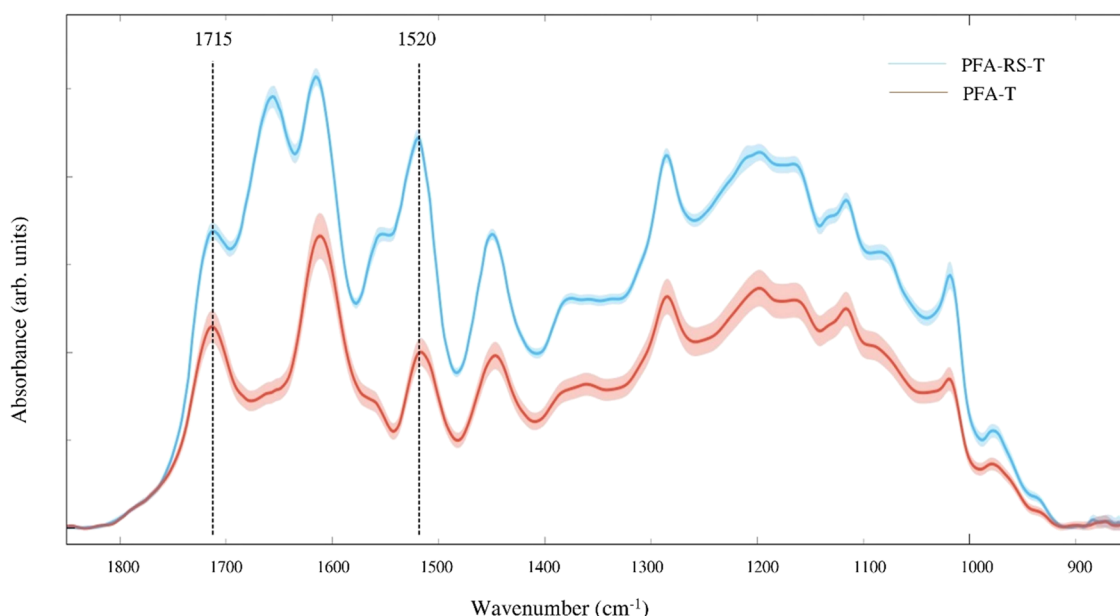


Figure 5. Average FTIR spectra of surface samples of polyfurfuryl alcohol-quebracho tannin (PFA-T, red curve) and polyfurfuryl alcohol-regenerated silk-quebracho tannin (PFA-RS-T, light blue curve).

both the formylated tannin (Figure S2 in Supporting Information section) and the Diels-Alder product. In order to obtain more information, two samples cross-linked in formic acid (PFA-T and PFA-RS-T) were analyzed, and the absorbance spectra obtained from FTIR imaging were compared. The relative analysis was compared, as reported in Figure 5.

The integration ratio between the peak at 1715 cm^{-1} ($\text{C}=\text{O}$) and at 1520 cm^{-1} ($\text{C}=\text{C}$ asymmetric stretching of tannin) is found to be 1.3 and 0.6 for PFA-T and PFA-RS-T, respectively, thus resulting in a decrease of more than 50% percent when RS is added to the PFA-tannin polymer.

This confirms that the addition of silk inhibits the Diels-Alder reaction, as reported in Scheme 2B. The protein chains fit into the polymer matrix by establishing secondary interactions, limiting the cross-linking to proceed. Due to the strong acidic environment, the formation of the covalent bonds between silk and furfuryl alcohol (proposed after ^{13}C -NMR observation) cannot be excluded, and the vibration of the $\text{CH}_2\text{-CH}$ proposed would be overlapped (stretching at around 3000 and bending at below 1000 cm^{-1}).

In relation to the intrinsic acidity of our formulation, it has to be noticed that despite no specific standard limits for the pH range of adhesives,⁶⁰ acid glues involve wood delamination.^{61,62} The formic acid applied for solubilizing the silk is involved also as an activator for the formylation of tannin and as a catalyst for furfuryl alcohol activation. Therefore, it is expected that free HCOOH is limited, and it can easily evaporate during the pressing stage. However, this aspect will be considered for future gluing durability study.

CONCLUSIONS

In this study, RS was successfully added to the tannin-furanic formulation to produce bio-based adhesives with enhanced mechanical properties. Significant enhancement of about 20–30% was observed in plywood gluing when 15–20 wt % of RS was added to the reference formulation in both dry and wet conditions.

These findings were rationalized considering that the presence of RS limits the cross-linking of the furanic polymer resulting in a homogeneous network in which the presence of chemical bonding between the silk and the furanic adduct is proposed.

This strategy provides an approach to develop formaldehyde-free bio-based wood adhesive with rapid preparation, excellent performance, and sustainability. It was shown that the combination between vegetal and animal bioresources can cooperate synergically for the production of performing wood adhesives. The interaction between silk, tannin, and furanics can also be considered for other applications in the field of material science, with particularly interesting perspectives in bio-plastic, construction composites, and automotive and also in medical and biological devices.

ASSOCIATED CONTENT

Supporting Information

The Supporting Information is available free of charge at <https://pubs.acs.org/doi/10.1021/acsapm.3c00539>.

SEM images of TFS-20 before and after solubilization into acid formic- CaCl_2 solution and relative chemical analysis and ATR-FTIR spectra of quebracho tannin powder (black curve) and leached quebracho tannin after reaction with formic acid at $100\text{ }^\circ\text{C}$ for 1 h (PDF)

AUTHOR INFORMATION

Corresponding Author

Gianluca Tondi – TESAF Land Environment Agriculture & Forestry Department, University of Padua, 35020 Legnaro, Italy; orcid.org/0000-0003-2383-6495; Phone: +39-049-8272776; Email: gianluca.tondi@unipd.it

Authors

Emanuele Cesprini – TESAF Land Environment Agriculture & Forestry Department, University of Padua, 35020 Legnaro, Italy; orcid.org/0000-0003-0543-3211

Johannes Jorda – Department of Green Engineering and Circular Design, Salzburg University of Applied Sciences, 5431 Kuchl, Austria

Marco Paolantoni – Department of Chemistry, Biology and Biotechnology, University of Perugia, 06123 Perugia, Italy; orcid.org/0000-0002-6266-3497

Luca Valentini – Civil and Environmental Engineering Department, University of Perugia, 05100 Terni, Italy; orcid.org/0000-0002-6803-5889

Primož Sket – Slovenian NMR Centre, National Institute of Chemistry, SI-1000 Ljubljana, Slovenia

Valerio Causin – Department of Chemical Sciences, University of Padua, 35131 Padova, Italy

Diana E. Bedolla – Elettra Sincrotrone Trieste, 34149 Basovizza, TS, Italia; Area Science Park, 34149 Padriciano, TS, Italia; orcid.org/0000-0003-1902-1517

Michela Zanetti – TESAF Land Environment Agriculture & Forestry Department, University of Padua, 35020 Legnaro, Italy

Complete contact information is available at: <https://pubs.acs.org/10.1021/acsapm.3c00539>

Author Contributions

The manuscript was written through contributions of all authors. All authors have given approval to the final version of the manuscript.

Notes

The authors declare no competing financial interest.

ACKNOWLEDGMENTS

G.T. gratefully acknowledges the TESAF dept. for supporting this research with BIRD 2021 fundings “Biocomby-“. E.C. thanks the LERH doctorate school for the grant financing his PhD. L.V. received funding from the Italian Ministry of Education, University and Research (MIUR) under the PRIN project “Development and promotion of the Levulinic acid and Carboxylate platforms by the formulation of advanced PHA-based biomaterials and their exploitation for 3D printed green-electronics applications” grant 2017FWC3WC. D.B. gratefully acknowledges the project Interreg ITAT 1059 InCIMA4 for supporting this study.

REFERENCES

- (1) Söderholm, P. The green economy transition: The challenges of technological change for sustainability. *Sustain. Earth* **2020**, *3*, 6.
- (2) CIEL. Plastic & Climate: The hidden costs of a plastic planet, 2019. <https://www.ciel.org/wp-content/uploads/2019/05/Plastic-and-Climate-FINAL-2019.pdf>.
- (3) Zheng, J.; Suh, S. Strategies to reduce the global carbon footprint of plastics. *Nat. Clim. Chang.* **2019**, *9*, 374–378.
- (4) Spierling, S.; Knüpfner, E.; Behnsen, H.; Mudersbach, M.; Krieg, H.; Springer, S.; Albrecht, S.; Herrmann, C.; Endres, H. J. Bio-Based Plastics - A review of environmental, social and economic impact assessments. *J. Clean. Prod.* **2018**, *185*, 476–491.
- (5) Rosenboom, J. G.; Langer, R.; Traverso, G. The hidden costs of a plastic planet. *Nat. Rev. Mater.* **2022**, *7*, 117–137.
- (6) Cesprini, E.; De Iseppi, A.; Giovando, S.; Tarabra, E.; Zanetti, M.; Sket, P.; Marangon, M.; Tondi, G. Chemical characterization of cherry (*Prunus Avium*) extract in comparison with commercial mimosa and chestnut tannins. *Wood Sci. Technol.* **2022**, *56*, 1455–1473.
- (7) Shirmohammadli, Y.; Efhamisizi, D.; Pizzi, A. Tannins as a sustainable raw material for green chemistry: A review. *Ind. Crops Prod.* **2018**, *126*, 316–332.

(8) Falcão, L.; Araújo, M. E. M. Vegetable tannins used in the manufacture of historic leathers. *Molecules* **2018**, *23*, 1081.

(9) Cook, N. C.; Samman, S. Flavonoids - chemistry, metabolism, cardioprotective effects, and dietary Sources. *J. Nutr. Biochem.* **1996**, *7*, 66–76.

(10) Eckardt, J.; Neubauer, J.; Sepperer, T.; Donato, S.; Zanetti, M.; Cefarin, N.; Vaccari, L.; Lippert, M.; Wind, M.; Schnabel, T.; Petutschnigg, A.; Tondi, G. Synthesis and characterization of high-performing sulfur-free tannin foams. *Polymers (Basel)* **2020**, *12*, 564.

(11) Tondi, G.; Pizzi, A. Tannin-based rigid foams: characterization and modification. *Ind. Crops Prod.* **2009**, *29*, 356–363.

(12) Arbenz, A.; Avérous, L. Chemical modification of tannins to elaborate aromatic biobased macromolecular architectures. *Green Chem.* **2015**, *17*, 2626–2646.

(13) Sommerauer, L.; Thevenon, M. F.; Petutschnigg, A.; Tondi, G. Effect of hardening parameters of wood preservatives based on tannin copolymers. *Holzforschung* **2019**, *73*, 457–467.

(14) Cesprini, E.; Baccini, R.; Urso, T.; Zanetti, M.; Tondi, G. Quebracho-based wood preservatives: effect of concentration and hardener on timber properties. *Coatings* **2022**, *12*, 568.

(15) Pizzi, A. Recent developments in eco-efficient bio-based adhesives for wood bonding: Opportunities and issues. *J. Adhes. Sci. Technol.* **2006**, *20*, 829–846.

(16) Hemmilä, V.; Adamopoulos, S.; Karlsson, O.; Kumar, A. Development of sustainable bio-adhesives for engineered wood panels-A review. *RSC Adv.* **2017**, *7*, 38604–38630.

(17) Pizzi, A. Tannins: Prospectives and actual industrial applications. *Biomolecules* **2019**, *9*, 344.

(18) Tondi, G. Tannin-based copolymer resins: Synthesis and characterization by solid state ¹³C NMR and FT-IR spectroscopy. *Polymers (Basel)* **2017**, *9*, 223.

(19) Gandini, A. Polymers from renewable resources: a challenge for the future of macromolecular materials. *Macromolecules* **2008**, *41*, 9491–9504.

(20) Choura, M.; Belgacem, N. M.; Gandini, A. The acid-catalyzed polycondensation of furfuryl alcohol: old puzzles unravelled. *Macromol. Symp.* **1997**, *122*, 263–268.

(21) Choura, M.; Belgacem, N. M.; Gandini, A. Acid-catalyzed polycondensation of furfuryl alcohol: mechanisms of chromophore formation and cross-linking. *Macromolecules* **1996**, *29*, 3839–3850.

(22) Pfriem, A.; Dietrich, T.; Buchelt, B. furfuryl alcohol impregnation for improved plasticization and fixation during the densification of wood. *Holzforschung* **2012**, *66*, 215–218.

(23) Kong, L.; Guan, H.; Wang, X. In situ polymerization of furfuryl alcohol with ammonium dihydrogen phosphate in poplar wood for improved dimensional stability and flame retardancy. *ACS Sustainable Chem. Eng.* **2018**, *6*, 3349–3357.

(24) Yao, M.; Yang, Y.; Song, J.; Yu, Y.; Jin, Y. Lignin-based catalysts for chinese fir furfurylation to improve dimensional stability and mechanical properties. *Ind. Crops Prod.* **2017**, *107*, 38–44.

(25) Falco, G.; Guigo, N.; Vincent, L.; Sbirrazzuoli, N. Opening furan for tailoring properties of bio-based poly(furfuryl alcohol) thermoset. *ChemSusChem* **2018**, *11*, 1805–1812.

(26) Luckeneder, P.; Gavino, J.; Kuchernig, R.; Petutschnigg, A.; Tondi, G. Sustainable phenolic fractions as basis for furfuryl alcohol-based co-polymers and their use as wood adhesives. *Polymers (Basel)* **2016**, *8*, 396.

(27) Szcurek, A.; Fierro, V.; Thébault, M.; Pizzi, A.; Celzard, A. Structure and properties of poly(furfuryl alcohol)-tannin polyHIPes. *Eur. Polym. J.* **2016**, *78*, 195–212.

(28) Cesprini, E.; Causin, V.; De Iseppi, A.; Zanetti, M.; Marangon, M.; Barbu, M. C.; Tondi, G. Renewable tannin-based adhesive from Quebracho extract and furfural for particleboards. *Forests* **2022**, *13*, 1781.

(29) Jorda, J.; Cesprini, E.; Barbu, M.-C.; Tondi, G.; Zanetti, M.; Král, P. Quebracho tannin bio-based adhesives for plywood. *Polymers (Basel)* **2022**, *14*, 2257.

(30) Zhang, J.; Long, C.; Zhang, X.; Liu, Z.; Zhang, X.; Liu, T.; Li, J.; Gao, Q. An easy-coating, versatile, and strong soy flour adhesive via a

biomineralized structure combined with a biomimetic brush-like polymer. *Chem. Eng. J.* **2022**, *450*, No. 138387.

(31) Xu, Y.; Han, Y.; Li, J.; Luo, J.; Shi, S. Q.; Li, J.; Gao, Q.; Mao, A. Research progress of soybean protein adhesive: a review. *J. Renew. Mater.* **2022**, *10*, 2519–2541.

(32) Chen, X.; Yang, Z.; Yang, F.; Pizzi, A.; Essawy, H.; Du, G.; Zhou, X. Development of easy-handling, formaldehyde-free, high-bonding performance bio-sourced wood adhesives by co-reaction of furfuryl alcohol and wheat gluten protein. *Chem. Eng. J.* **2023**, *462*, No. 142161.

(33) Zhao, X.; Liu, T.; Ou, R.; Hao, X.; Fan, Q.; Guo, C.; Sun, L.; Liu, Z.; Wang, Q. Fully Biobased Soy Protein Adhesives with Integrated High-Strength, Waterproof, Mildew-Resistant, and Flame-Retardant Properties. *ACS Sustainable Chem. Eng.* **2022**, *10*, 6675–6686.

(34) Cao, Z.; Chen, X.; Yao, J.; Huang, L.; Shao, Z. The preparation of regenerated silk fibroin microspheres. *Soft Matter* **2007**, *3*, 910–915.

(35) Ceccarini, M. R.; Palazzi, V.; Salvati, R.; Chiesa, I.; De Maria, C.; Bonafoni, S.; Mezzanotte, P.; Codini, M.; Pacini, L.; Errante, F.; Rovero, P.; Morabito, A.; Beccari, T.; Roselli, L.; Valentini, L. Biomaterial inks from peptide-functionalized silk fibers for 3D printing of futuristic wound-healing and sensing materials. *Int. J. Mol. Sci.* **2023**, *24*, 947.

(36) Santoni, I.; Pizzo, B. Evaluation of alternative vegetable proteins as wood adhesives. *Ind. Crops Prod.* **2013**, *45*, 148–154.

(37) Raydan, N. D. V.; Leroyer, L.; Charrier, B.; Robles, E. Recent advances on the development of protein-based adhesives for wood composite materials—a review. *Molecules* **2021**, *26*, 7617.

(38) Valentini, L.; Ceccarini, M. R.; Verdejo, R.; Tondi, G.; Beccari, T. Stretchable, bio-compatible, antioxidant and self-powering adhesives from soluble silk fibroin and vegetal polyphenols exfoliated graphite. *Nanomaterials* **2021**, *11*, 2352.

(39) British Standards, E. B. *Plywood — Bonding Quality — EN 314-1:2004*, 2004, 3.

(40) British Standards, E. B. *Wood-Based Panels — Determination of Modulus of Elasticity in Bending and of Bending Strength-EN 310:1993*, 1993, 1–14.

(41) Toplak, M.; Read, S. T.; Sandt, C.; Borondics, F. Quasar: easy machine learning for biospectroscopy. *Cell* **2021**, *10*, 2300.

(42) Toplak, M.; Birarda, G.; Read, S.; Sandt, C.; Rosendahl, S. M.; Vaccari, L.; Demšar, J.; Borondics, F. Infrared orange: connecting hyperspectral data with machine learning. *Synchrotron Radiat. News* **2017**, *30*, 40–45.

(43) Xi, X.; Pizzi, A.; Frihart, C. R.; Lorenz, L.; Gerardin, C. Tannin plywood bioadhesives with non-volatile aldehydes generation by specific oxidation of mono- and disaccharides. *Int. J. Adhes. Adhes.* **2020**, *98*, No. 102499.

(44) Liu, Z.; Chen, M.; Xu, Y.; Zhang, J.; Huang, X.; Luo, J.; Li, J.; Shi, S. Q.; Gao, Q. Preparation of a strong and multiple-function soybean flour adhesive via the construction of tannin microspheres with a core-shell structure. *Compos. Part B Eng.* **2022**, *242*, No. 110114.

(45) Zhou, Y.; Zeng, G.; Zhang, F.; Tang, Z.; Luo, J.; Li, K.; Li, X.; Li, J.; Shi, S. Q. Preparation of functional fiber hybrid enhanced high strength and multifunctional protein based adhesive. *Mater. Des.* **2022**, *224*, No. 111289.

(46) Pang, H.; Zhao, S.; Mo, L.; Wang, Z.; Zhang, W.; Huang, A.; Zhang, S.; Li, J. Mussel-inspired bio-based water-resistant soy adhesives with low-cost dopamine analogue-modified silkworm silk fiber. *J. Appl. Polym. Sci.* **2020**, *137*, 48785.

(47) Liu, Z.; Liu, T.; Jiang, H.; Zhang, X.; Li, J.; Shi, S. Q.; Gao, Q. Biomimetic lignin-protein adhesive with dynamic covalent/hydrogen hybrid networks enables high bonding performance and wood-based panel recycling. *Int. J. Biol. Macromol.* **2022**, *214*, 230–240.

(48) Hafiz, N. L. M.; Tahir, P. M. D.; Hua, L. S.; Abidin, Z. Z.; Sabaruddin, F. A.; Yunus, N. M.; Abdullah, U. H.; Abdul Khalil, H. P. S. Curing and thermal properties of co-polymerized tannin phenol-

formaldehyde resin for bonding wood veneers. *J. Mater. Res. Technol.* **2020**, *9*, 6994–7001.

(49) Jorda, J.; Kain, G.; Barbu, M. C.; Petutschnigg, A.; Král, P. Influence of adhesive systems on the mechanical and physical properties of flax fiber reinforced beech plywood. *Polymers (Basel)* **2021**, *13*, 3086.

(50) Biadala, T.; Czarnecki, R.; Dukarska, D. Water resistant plywood of increased elasticity produced from european wood species. *Wood Res.* **2020**, *65*, 111–124.

(51) Lei, H.; Frazier, C. E. Curing behavior of melamine-urea-formaldehyde (MUF) resin adhesive. *Int. J. Adhes. Adhes.* **2015**, *62*, 40–44.

(52) Cefarin, N.; Bedolla, D. E.; Surowka, A.; Donato, S.; Sepperer, T.; Tondi, G.; Dreossi, D.; Sodini, N.; Birarda, G.; Vaccari, L. Study of the spatio-chemical heterogeneity of tannin-furanic foams: From 1D FTIR spectroscopy to 3D FTIR micro-computed tomography. *Int. J. Mol. Sci.* **2021**, *22*, 12869.

(53) Cesprini, E.; Šket, P.; Causin, V.; Zanetti, M.; Tondi, G. Development of Quebracho (*Schinopsis Balansae*) tannin-based thermoset resins. *Polymers (Basel)* **2021**, *13*, 4412.

(54) Conley, R.; Metil, I. *An investigation of the structure of furfuryl alcohol polycondensates with infrared spectroscopy*; Reinhold Publishing Corporation: New York, 1963.

(55) Myers, G. E. ¹³C NMR Study of curing in furfuryl alcohol resins. *Macromolecules* **1984**, *17*, 1087–1090.

(56) Tondi, G.; Cefarin, N.; Sepperer, T.; D'Amico, F.; Berger, R. J. F.; Musso, M.; Birarda, G.; Reyer, A.; Schnabel, T.; Vaccari, L. Understanding the polymerization of polyfurfuryl alcohol: ring opening and Diels-Alder reactions. *Polymers (Basel)* **2019**, *11*, 2126.

(57) D'Amico, F.; Musso, M. E.; Berger, R. J. F.; Cefarin, N.; Birarda, G.; Tondi, G.; Bertoldo Menezes, D.; Reyer, A.; Scarabattoli, L.; Sepperer, T.; Schnabel, T.; Vaccari, L. Chemical constitution of polyfurfuryl alcohol investigated by FTIR and resonant Raman spectroscopy. *Spectrochim. Acta A Mol. Biomol. Spectrosc.* **2021**, *262*, No. 120090.

(58) Buchwalter, S. L. Polymerization of furfuryl acetate in acetone/nitro. *J. Polym. Sci. Polym. Chem. Ed.* **1985**, *23*, 2897–2911.

(59) Ma, M.; Dong, S.; Hussain, M.; Zhou, W. Effects of addition of condensed tannin on the structure and properties of silk fibroin film. *Polym. Int.* **2017**, *66*, 151–159.

(60) Simon, F.; Legrand, G. Overview of European standards for adhesives used in wood-based products. *J. Adhes. Sci. Technol.* **2010**, *24*, 1611–1627.

(61) Alade, A. A.; Naghizadeh, Z.; Wessels, C. B.; Tyhoda, L. A review of the effects of wood preservative impregnation on adhesive bonding and joint performance. *J. Adhes. Sci. Technol.* **2022**, *36*, 1593–1617.

(62) Zanetti, M.; Pizzi, A. Upgrading of MUF polycondensation resins by buffering additives. II. hexamine sulfate mechanisms and alternate buffers. *J. Appl. Polym. Sci.* **2003**, *90*, 215–226.